

Exploring the possible role of hybridization in the evolution of photosynthetic pathways in *Flaveria* (Asteraceae), the prime model of C₄ photosynthesis evolution

Diego F. Morales-Briones^{1*} and Gudrun Kadereit^{1*}

¹ Princess Therese von Bayern chair of Systematics, Biodiversity and Evolution of Plants, Ludwig-Maximilians-Universität München, Munich, Germany.

* Correspondence:

Gudrun Kadereit

g.kadereit@biologie.uni-muenchen.de

Diego F. Morales-Briones

dfmoralesb@gmail.com

Abstract

Flaveria (Asteraceae) is the prime model for the study of C₄ photosynthesis evolution and seems to support a stepwise acquisition of the pathway through C₃-C₄ intermediate phenotypes, still existing in *Flaveria* today. Molecular phylogenies of *Flaveria* based on concatenated data matrices are currently used to reconstruct the complex sequence of trait shifts during C₄ evolution. To assess the possible role of hybridization in C₄ evolution in *Flaveria*, we re-analyzed transcriptome data of 17 *Flaveria* species to infer the extent of gene tree discordance and possible reticulation events. We found massive gene tree discordance as well as reticulation along the backbone and within clades containing C₃-C₄ intermediate and C₄-like species. An early hybridization event between two C₃ species might have triggered C₄ evolution in the genus. The clade containing all C₄ species plus the C₄-like species *F. vaginata* and *F. palmeri* is robust but of hybrid origin involving *F. angustifolia* and *F. sonorensis* (both C₃-C₄ intermediate) as parental lineages. Hybridization seems to be a driver of C₄ evolution in *Flaveria* and likely promoted the fast acquisition of C₄ traits. This new insight can be used in further exploring C₄ evolution and can inform C₄ bioengineering efforts.

Keywords: C₃-C₄ intermediates; C₄ photosynthesis evolution; Hybridization; HyDe analysis; RNA-Seq; Reticulate evolution; Species network analysis.

INTRODUCTION

The detection of gene tree discordance is common in the phylogenomic era. Discordance can be the product of multiple processes and is commonly attributed to either incomplete lineage sorting (ILS) and/or hybridization (Pamilo and Nei, 1988; Doyle, 1992; Galtier and Daubin, 2008). Hybridization is a fundamental process in the evolution of animals, plants, and fungi (Giraud et al., 2008; Schwenk et al., 2008; Soltis and Soltis, 2009; Payseur and Rieseberg, 2016), and methods to investigate hybridization in a phylogenetic context recently have been developed greatly. These include methods that estimate phylogenetic networks while accounting for ILS and hybridization simultaneously (e.g., Solís-Lemus and Ané, 2016; Wen et al., 2018), and methods that detect hybridization based on site patterns or phylogenetic invariants (e.g., Green et al., 2010; Durand et al., 2011; Kubatko and Chifman, 2019). The current ease to produce phylogenomic data sets and the availability of new analytical methods facilitate the exploration of reticulate evolution in any clade across the Tree of Life, including those that have particular significance as model lineages, such as the flowering plant genus *Flaveria* (Asteraceae) for the study of C₄ photosynthesis evolution.

Flaveria belongs to the sunflower tribe Heliantheae (Anderberg et al., 2007). According to the most recent revision by Powell (1978), *Flaveria* includes 21 morphologically rather similar species distributed mainly in southern USA and northern Mexico, with few species occurring in the Caribbean and South America. The two weedy and self-compatible C₄ species, *F. trinervia* and *F. bidentis*, have been introduced almost worldwide (<https://powo.science.kew.org/>). Species of *Flaveria* usually show scattered occurrences in unconnected, localized populations near rivers, creeks, irrigation canals, fields, roadsides, and ponds, often on saline or gypseous soils (Powell, 1978). They are either robust shrubs or

herbaceous perennials, or annuals (mainly the C₄ species). The genus stands out in Asteraceae for its reduced floral features and reduced and secondarily aggregated capitula (Anderberg et al., 2007). Reduction is most evident in *F. trinervia* (C₄) and aggregation of capitula mimicking a single capitulum in *F. anomala* (C₃-C₄). *Flaveria* is consistently diploid (see Powell, 1978 and ref. therein; only exceptions are some tetraploid populations of *F. pringlei*) with a haploid chromosome number of $n = 18$. Artificial hybridization among 16 species of *Flaveria* was successful, and F1 hybrids could be obtained in most species' combinations (see Table 1 in Powell, 1978). F2 and backcross crosses also resulted in offspring in a high number of combinations, but only four of these were fertile. Powell (1978) excluded frequent natural hybridization in *Flaveria* mainly because of geographical isolation.

C₄ photosynthesis in *Flaveria* was first recognized by Smith and Turner (1975), and the presence of C₃-C₄ intermediate species was first noted by Brown (pers. comm. in Powell, 1978), first verified by Apel and Maass (1981) and then studied in detail biochemically in four species by Ku et al. (1983) and Nakamoto et al. (1983). Numerous publications characterizing the physiology and biochemistry of C₃-C₄ intermediate species of *Flaveria* followed (Ku et al., 1991 and ref. therein). At the same time crossing experiments of C₃ and C₄ *Flaveria* species as well as backcrosses or crosses between C₃-C₄ intermediate species revealed the transfer of C₄ properties as well as the simultaneous functioning of C₃ and C₄ pathways in hybrids (see Apel et al., 1988 as an example and Kadereit et al., 2017 for review). Of all genera that contain C₃-C₄ intermediate species, *Flaveria* has the highest diversity of C₃-C₄ phenotypes including C₂ photosynthesis (Sage et al., 2012; briefly described in Table 1), and arguably is the only lineage that allows to infer a detailed sequence of increasing C₄-ness (Sage et al., 2012). Against this background, *Flaveria* qualified as the model group for the establishment (Monson and Moore, 1989) and

subsequent refinement of a model of stepwise acquisition of C₄ photosynthesis through intermediate steps (Sage et al., 2014 and ref. therein).

One challenge of the *Flaveria* model is that C₃-C₄ intermediate phenotypes might also have resulted from reticulation during the diversification of the genus, especially when reproductive barriers are leaky among extant species as soon as they get into contact (Powell, 1978) and hybridization between C₃ and C₄ species is possible. Therefore, a phylogenetic study exploring the occurrence and location of past reticulation events is needed. Comprehensive molecular phylogenetic studies of *Flaveria* published so far were either based on few molecular markers only (McKown et al., 2005), or on concatenated data matrices and inference methods unable to reveal tree discordance, possible reticulation, or incomplete lineage sorting (Lyu et al., 2015). Irrespective of this, numerous current studies of evolutionary change during the establishment of the C₄ pathway rely on the *Flaveria* model (e.g., Lyu et al., 2021; Taniguchi et al., 2021).

The aim of this study is to use available transcriptome data of 17 species of *Flaveria* to assess the extent of reticulation during the diversification of the genus, and to evaluate these findings with respect to the evolution of C₄ photosynthesis in the genus and its suitability as general model of C₄ evolution.

Table 1. Photosynthetic types in *Flaveria* according to Sage et al. (2014 and 2018 and ref. therein); species names marked * were not sampled in this study, mesophyll (M), bundle sheath (BS), glycine decarboxylase (GDC).

Photosynthetic type	Characteristics	<i>Flaveria</i> species representing this type ¹
C ₃	Photorespiratory cycle operates completely within single M cells, BS cells small ² with few organelles, veins widely spaced	<i>F. cronquistii</i> ² , <i>F. mcdougallii</i> *
C ₃ proto-kranz	Functionally C ₃ , activated BS cells, greater vein density, mitochondria localized at the inner BS wall adjacent to the vasculature	<i>F. pringlei</i> , <i>F. robusta</i>
C ₂ Type I	Low or no GDC expression in M cells, high number of centripetally located organelles in the BS cells, CO ₂ compensation point reduced in comparison to C ₃ , lack of any C ₄ cycle	<i>F. angustifolia</i> , <i>F. chlorifolia</i> , <i>F. sonorensis</i>
C ₂ Type II	In addition to type I, modest C ₄ cycle enhancement	<i>F. anomala</i> , <i>F. floridana</i> , <i>F. linearis</i> *, <i>F. pubescens</i> , <i>F. ramosissima</i>
C ₄ -like	Strong C ₄ metabolic cycle but also weak C ₃ cycle in the M cells	<i>F. brownii</i> , <i>F. palmeri</i> , <i>F. vaginata</i>
C ₄	No C ₃ cycle, CO ₂ -saturate photosynthesis below 500 ppm CO ₂	<i>F. bidentis</i> , <i>F. campestre</i> *, <i>F. kochiana</i> , <i>F. trinervia</i> , <i>F. australasica</i> ,

¹ *Flaveria oppositifolia** so far only classified as C₂ without further specification.

² *Flaveria cronquistii* qualifies as a C₃+ species (see Sage et al., 2018) because it has larger and photosynthetically more active BS cells (McKown and Dengler, 2007).

MATERIAL AND METHODS

Taxon sampling

We included publicly available transcriptomes from 17 species of *Flaveria* (Table S1). In addition, we included outgroups from four genomes of Asteraceae (*Chrysanthemum*, *Helianthus*, *Lactuca* and *Stevia*) following (Mandel et al., 2019; Table S1).

Homology and orthology inference

Raw read processing, transcriptome assembly, low-quality and chimeric transcript removal, transcript clustering into putative genes, translation, and final coding sequences (CDS) redundancy assessment were carried out following Morales-Briones et al. (2021) with minor modifications as follows. Sequencing errors in raw reads were corrected with Rcorrector (Song and Florea, 2015) and reads flagged as uncorrectable were discarded. Sequencing adapters and low-quality bases were removed with Trimmomatic v 0.39 (Bolger et al., 2014). Additionally, chloroplast and mitochondrial reads were filtered out with Bowtie2 v 2.4.4 (Langmead and Salzberg, 2012) using publicly available Asterales organelle genomes from the Organelle Genome Resources database (RefSeq; [Pruitt et al., 2007]; last accessed on June 4, 2021) as references. Read quality was assessed with FastQC v 0.11.9 (<http://www.bioinformatics.bbsrc.ac.uk/projects/fastqc>) and overrepresented sequences were discarded. *De novo* assembly was carried out with Trinity v 2.13.2 (Grabherr et al., 2011) with default settings, but without in silico normalization. Assembly quality was assessed with Transrate v 1.0.3 (Smith-Unna et al., 2016). Low quality and poorly supported transcripts were removed using individual cut-off values for three contig score components of Transrate: 1) proportion of nucleotides in a contig that agrees in identity with the aligned read, $s(\text{Cnuc}) \leq 0.25$;

2) proportion of nucleotides in a contig that have one or more mapped reads, $s(\text{Ccov}) \leq 0.25$; and
 3) proportion of reads that map to the contig in correct orientation, $s(\text{Cord}) \leq 0.5$. Furthermore,
 chimeric transcripts (*trans*-self and *trans*-multi-gene) were removed following the approach
 described in Yang and Smith (2013) using *Helianthus annuus* as the reference proteome, and a
 percentage similarity and length cutoff of 30 and 100, respectively. To remove isoforms and
 assembly artifacts, filtered reads were remapped to filtered transcripts with Salmon v 1.5.2 (Patro
 et al., 2017) and putative genes were clustered with Corset v 1.09 (Davidson and Oshlack, 2014)
 using default settings, except that we used a minimum of five reads as threshold to remove
 transcripts with low coverage ($-m\ 5$). Only the longest transcript of each putative gene inferred
 by Corset was retained as suggested in Chen et al. (2019). Filtered transcripts were translated
 with TransDecoder v 5.3.0 (Haas et al., 2013) with default settings and the proteomes of
Arabidopsis thaliana, *Helianthus annuus*, and *Lactuca sativa* to identify open reading frames.
 Finally, coding sequences (CDS) from translated amino acids were further reduced with CD-HIT
 v 4.8.1 ($-c\ 0.99$; [Fu et al., 2012]) to remove near-identical sequences. Scripts used can be found
 at https://bitbucket.org/yanglab/phylogenomic_dataset_construction/src/master/ (Morales-
 Briones et al., 2021).

Homology inference was done with an all-by-all BLASTN search on CDS with an *E*
 value cutoff of 10. BLAST hits were filtered with a minimal hit coverage of 40%. Homolog
 groups were clustered with MCL v 14-137 (van Dongen, 2000) using a minimum minus log-
 transformed *E* value cutoff of 5 and an inflation value of 1.4, and only clusters with at least 17
 taxa were retained. Homolog cluster sequences were aligned using the OMM_MACSE v 11.05
 pipeline (Scornavacca et al., 2019). Alignments were further trimmed to remove columns with
 more than 90% missing data using Phyx (Brown et al., 2017). Homolog trees were inferred using

RAxML v 8.2.11 (Stamatakis, 2014) with the GTRCAT model and 200 rapid bootstrap (BS) replicates. Monophyletic and paraphyletic tips of the same species were removed, keeping the tip with the highest number of characters in the trimmed alignment following Yang and Smith (2014). Spurious tips were detected and removed using TreeShrink v 1.3.9 (Mai and Mirarab, 2018) with the 'per-gene' mode, a false positive error rate threshold (α) of 0.05, and excluding the outgroups. Trees were visually inspected, and deep paralogs producing internal branch lengths longer than 0.20 were cut apart retaining subclades with at least 10 taxa to obtain final homolog trees. Orthology inference was done using the 'monophyletic outgroup' (MO) approach from Yang and Smith (2014). The MO approach filters for trees that have outgroup taxa being monophyletic and single-copy, and therefore filters for single- and low-copy genes. This approach roots the gene tree by the outgroups, traverses the rooted tree from root to tip, and removes the side with less taxa when gene duplication is detected (Yang and Smith, 2014). If no taxon duplication is detected in a homolog tree, the MO approach outputs a one-to-one ortholog. We set all species of *Flaveria* as ingroups, and *Chrysanthemum*, *Helianthus*, *Lactuca*, and *Stevia* as outgroups, keeping orthologs that included at least 10 taxa.

Tree inference and detection of gene tree conflict

Sequences from individual orthologs were aligned using the OMM_MACSE pipeline. Columns with more than 20% missing data were trimmed with Phyx, and only alignments with at least 500 characters and all 21 taxa were retained and concatenated. We estimated a maximum likelihood (ML) tree of the concatenated matrix with IQ-TREE v 2.1.3 (Minh et al., 2020) searching for the best partition scheme (Lanfear et al., 2012) followed by ML gene tree inference and 1000 ultrafast bootstrap replicates for clade support. To estimate a coalescent-based species

tree, first, we inferred individual gene trees with IQ-TREE using extended model selection (Kalyaanamoorthy et al., 2017) and 200 non-parametric bootstrap replicates for clade support. Gene trees were then used to infer a species tree with ASTRAL-III v 5.7.7 (Zhang et al., 2018) using local posterior probabilities (LPP; Sayyari and Mirarab, 2016) to assess clade support.

We explored gene tree discordance by calculating the number of concordant and discordant bipartitions on each node of the concatenated and ASTRAL trees using Phyparts (Smith et al., 2015). We used individual gene trees with BS support of at least 50% for each node. Additionally, to distinguish conflict from poorly supported branches, we carried out a Quartet Sampling (QS; Pease et al., 2018) analysis using the concatenated matrix with a partition by gene (--genetrees), the concatenated IQ-TREE and ASTRAL trees, and 1000 replicates. To further visualize gene tree conflict, we built a cloudogram with the DensiTree function from Phangorn v 2.7.1 (Schliep, 2011) in R (R Core Team 2021). We first time-calibrated individual ortholog gene trees, for visualization purposes only, with TreePL v 1.0 (Smith and O'Meara, 2012). The most recent common ancestor (MRCA) of *Helianthus* and *Flaveria* was fixed to 21.5 MYA, and the MRCA of *Flaveria* was fixed to 4.3 MYA based on Mandel et al. (2019).

Testing for potential reticulation

First, to investigate if gene tree discordance can be explained by ILS alone, we performed coalescent simulations like Cloutier et al. (2019). An ultrametric tree with branch lengths in mutational units (μT) was inferred with PAUP v 4.0a (build 168; Swofford, 2002) by constraining a ML tree search to the ASTRAL tree and using the concatenated alignment, a GTRGAMMA model, and enforcing a strict molecular clock. The mutational branch lengths from the constrained tree and branch lengths in coalescent units ($\tau = T/4N_e$) from the ASTRAL

tree were used to estimate the population size parameter theta ($\Theta = \mu T/\tau$; Degnan and Rosenberg, 2009) for internal branches. Terminal branches were set with $\Theta = 1$. We then used Phybase v 1.4 (Liu and Yu, 2010), that implements the formula from Rannala and Yang (2003), to simulate 10,000 gene trees using the constraint tree and the estimated theta values. Lastly, we calculated the distribution of Robinson and Foulds (1981) tree-to-tree distances between the ASTRAL tree and each original gene tree using Phangorn and compared this with the distribution of tree-to-tree distances between the ASTRAL tree and the simulated gene trees.

To test for potential reticulation, we inferred species networks using maximum pseudo-likelihood (Yu and Nakhleh, 2015) in PhyloNet v 3.8.2 (Than et al., 2008) with the command “InferNetworks_MPL” and using individual ML gene trees as input. We included all 17 species of *Flaveria* and *Helianthus* as an outgroup (18-taxon data set). Network searches were performed allowing for up to ten reticulation events and using only nodes in the gene trees that have BS \geq 50%. To find the network with optimal number of reticulations, we plotted the number of reticulations versus the pseudo-likelihood score to determine when the score stabilizes (Blair and Ané, 2020). Given that the pseudo-likelihood scores did not stabilize after networks with ten reticulation events (see results) and to reduce network complexity, we performed one additional round of searches by removing taxa involved in reticulation from the previous search. We removed *F. brownii* (C₄-like) and *F. pringlei* (C₃; 16-taxon data set). These two species were inferred to be product of reticulation events in all ten original searches and were not involved in additional reticulation events (i.e., they are not a parental lineage of other reticulation events; see results). Network searches for the reduced data set were carried out similarly as with the original data set.

Additionally, we tested for hybridization with HyDe (Blischak et al., 2018), which uses site pattern frequencies (Kubatko and Chifman, 2019) to quantify the hybridization parameter γ between two parental lineages that form a hybrid lineage. We tested all triplet combinations using the ‘run_hyde.py’ script, the concatenated alignment, and a mapping file to assign species. Test significance was assessed with a Bonferroni correction ($\alpha = 0.05$) for the number of hypothesis tests conducted with estimates of γ between 0 and 1 (Blischak et al., 2018). We carried out HyDe hybridization test using all species and without *F. pringlei* (C₃), as it has been identified as a potential artificial hybrid (Lyu et al., 2015).

Assessment of whole genome duplication

To investigate potential whole genome duplication, product of reticulation events in *Flaveria* (see results), we mapped gene duplication events onto the inferred species tree following (Yang et al., 2018). First, we extracted rooted ingroup clades (orthogroup) from the final homolog trees by requiring at least 15 taxa and only orthogroups with an average BS ≥ 50 were used for mapping. Then gene duplication events were then mapped onto the MRCA on the species tree when two or more taxa overlapped between the two daughter clades on the rooted ingroup clade. Each node on a species tree can be counted only once from each gene tree to avoid nested gene duplications inflating the number of recorded duplications (Yang et al., 2018). Orthogroup extraction and mapping were carried out using the scripts “extract_clades.py” and “map_dups_mrca.py” from <https://bitbucket.org/blackrim/clustering> (Yang et al., 2018).

RESULTS

Orthology inference and phylogenetic analysis

The final number of orthologs with at least ten species was 5,374 with a mean of 4,809 orthologs per species (Table S1). The number of orthologs that included all 21 species was 1,295. The concatenated matrix (≥ 500 bp per ortholog) consisted of 1,582,170 aligned columns with a character occupancy of 93% from 1,249 orthologs.

The topologies from the IQ-TREE and ASTRAL trees were similar and most nodes had maximum support (BS = 100, LPP = 100; Fig. 1; Fig. S1). The two trees only differed in the placement of *Flaveria bidentis* (C₄) which had lower support on both cases (Fig. 1; Fig. S1). *Flaveria cronquistii* (C₃), *F. robusta* (C₃) and *F. pringlei* (C₃) + *F. angustifolia* (C₃-C₄) formed a grade which is sister to Clade A + Clade B (clades names followed McKown et al., 2005). Clade A from IQ-TREE comprised the same species and relationships as in Lyu et al. (2015). *Flaveria ramosissima* (C₃-C₄) and *F. palmeri* (C₄-like) were successive sisters to *F. kochiana* (C₄) + *F. vaginata* (C₄-like) and the C₄ clade [(*F. bidentis*, *F. trinervia* + *F. australasica*); BS = 83]. The ASTRAL tree recovered *F. bidentis* (C₄) sister to *F. kochiana* (C₄) + *F. vaginata* (C₄-like; LLP = 0.96; Fig. S1). Clade B included the same species as in Lyu et al. (2015) but also included *F. sonorensis* (C₃-C₄). Our analyses recovered *F. brownii* (C₄-like) + *F. sonorensis* (C₃-C₄) as sister to the remaining species in Clade B. The remaining species, all C₃-C₄, had similar relationships as in Lyu et al. (2015) with *F. anomala* as sister to the clade *F. pubescens*, *F. chlorifolia* + *F. floridana*.

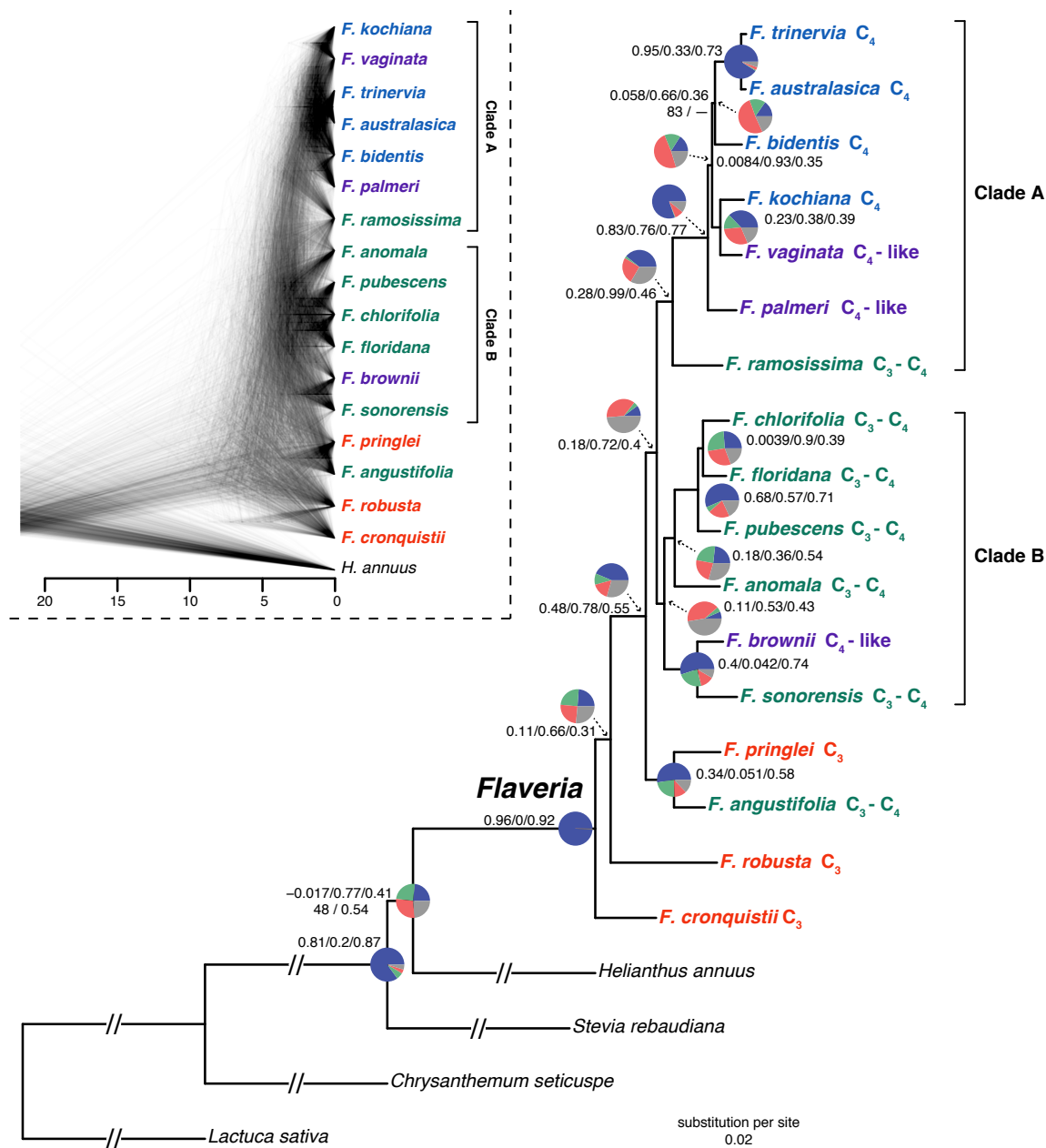


Fig. 1. Maximum likelihood phylogeny of *Flaveria* inferred with IQ-TREE from the concatenated 1249-nuclear gene supermatrix. Species names are colored by photosynthetic type. Quartet Sampling (QS) scores are shown above branches. QS scores: Quartet concordance/Quartet differential/Quartet informativeness. All nodes have full bootstrap support (BS =100) and local posterior probability (LLP =1) unless noted next to branches. Em dashes (—) denotes an alternative topology compared to the ASTRAL tree (Fig. S1). Pie charts represent the proportion of ortholog trees that support a clade (blue), the main alternative bifurcation (green), the remaining alternatives (red), and bifurcations (conflict or support) with <50% bootstrap support (gray). Branch lengths as number of substitutions per site (scale bar). Exceptionally long branches were shortened with a broken segment (/) for illustration purposes (See Fig. S1 for original branch lengths). Inset: Cloudogram inferred from 1288 nuclear ortholog trees. Scale in millions of years ago (MA).

Phylogenetic conflict

Overall, conflict analyses and cloudogram visualization revealed rampant gene tree discordance in *Flaveria* (Fig. 1; Fig S2). The cloudogram showed significant conflict along the backbone of the phylogeny as well as within clades A and B (Fig. 1). The placement of *F. robusta* (C₃) was supported only by 308 (of 947) informative gene trees and had low QS support (0.11/0.66/0.3) with a clear signal of an alternative topology involving *F. cronquistii*. The sister relationship of *F. pringlei* (C₃) and *F. angustifolia* (C₃-C₄) was supported by 677 (of 1,123) gene trees and had moderate QS support (0.34/0.051/0.58) and a strong signal of an alternative topology. The placement of *F. pringlei* (C₃) + *F. angustifolia* (C₃-C₄) as sister of Clade A + Clade B was supported by 562 (of 909) gene trees and had strong QS support (0.48/0.78/0.55) with moderate signal for an alternative topology. The clade composed of clades A and B was supported only by 131 (of 661) gene trees and had low QS support (0.18/0.72/0.4) but had no signals of an alternative topology. Clade A was supported by 505 (of 858) gene trees and had moderate QS support (0.28/0.99/0.46) but showed no signals of alternative topologies. The remaining species of Clade A [excluding *F. ramosissima* (C₃-C₄)] formed a clade supported by most gene trees (1,037 of 1,151) and a strong QS score (0.83/0.76/0.77) with no signals of an alternative topology. *Flaveria kochiana* (C₄) + *F. vaginata* (C₄-like) was supported by 479 (of 1,049) gene trees and had moderate QS support (0.23/0.38/0.39) with a clear signal of an alternative topology. *Flaveria trinervia* (C₄) + *F. australasica* (C₄) was supported by most gene trees (1,172 of 1,220) and had strong QS support with no signals of alternative topologies. *Flaveria bidentis* (C₄) as sister to *F. trinervia* (C₄) + *F. australasica* (C₄; IQ-TREE) was supported by 197 (of 1,054) and had very low QS support with a signal of an alternative topology. When *F. bidentis* (C₄) was placed as sister to *F. kochiana* (C₄) + *F. vaginata* (C₄-like;

ASTRAL) the clade formed by these three species was supported by even fewer gene trees (170 of 1,037) and QS counter-support (-0.027/0.72/0.38; Fig. S3). The clade composed of *F. kochiana* (C₄) + *F. vaginata* (C₄-like) and the C₄ clade *F. bidentis*, *F. trinervia* + *F. australasica* was supported by 206 (of 1,028) gene trees and had very low QS support (0.0084/0.93/0.35) with signals of alternative topologies. Clade B was supported by only 85 (of 679) gene trees and had low QS support (0.11/0.53/0.43) with signals of an alternative topology. *Flaveria brownii* (C₄-like) + *F. sonorensis* (C₃-C₄) was supported by 708 (of 1,180) gene trees and had moderate QS support (0.4/0.042/0.74) with clear signals of an alternative topology. The four remaining species of Clade B formed a clade supported by 299 (of 910) gene trees and had low QS support (0.11/0.53/0.43) with signals of an alternative topology. *Flaveria chlorifolia* (C₃-C₄) + *F. floridana* (C₃-C₄) was supported by 337 (of 1,042) gene trees and had very low QS support (0.0039/0.9/0.39) with clear signals of an alternative topology. Lastly, the C₃-C₄ clade (*F. pubescens*, *F. chlorifolia* + *F. floridana*) was supported by 727 (of 1,055) gene trees and had strong QS support (0.68/0.57/0.71) with a slight signal of an alternative topology.

Potential widespread reticulation

The distribution of tree-to-tree distances of the empirical and simulated gene trees to the ASTRAL tree showed some overlap (Fig. S4), but there was a skew towards larger distances in the empirical trees (mean 16.61) compared to distances in the simulated trees (mean 11.80). This suggested that ILS alone cannot explain most of the observed gene tree incongruence (Maureira-Butler et al., 2008).

Species network analyses recovered topologies with up to ten reticulations events for the 18-taxon data set (Fig. S6). The pseudo-likelihood score (Fig. S5) continually improved with the inclusion of additional reticulation events, and the network with ten reticulations (Fig. 2A) had the best score. Although the best-scored network showed complicated and nested reticulation patterns (Fig. 2A), there are several clear patterns among most networks (Fig. S6). *Flaveria brownii* (C₄-like) and *F. pringlei* (C₃) were consistently recovered as hybrids in all ten networks (Fig. S6). In both cases, parental lineages and inheritance probabilities were consistent across networks. Other reticulation patterns recovered across networks were the hybrid origin of clades A (mainly C₄ and C₄-like) and B (mainly C₃-C₄), which both had *F. sonorensis* (C₃-C₄; itself a hybrid in some networks) and *F. angustifolia* (C₃-C₄; or closely related to lineage) as potential parental lineages. The last reticulation event recovered in all networks involved the C₃ species *F. cronquistii* and *F. robusta* which were potential parental lineages of all remaining *Flaveria* species. The analyses of the 16-taxon data set (Fig. S6) resulted in a best-scoring network with five reticulation events (Fig. 2B). This showed patterns like the 18-taxon dataset regarding the hybrid origin of clades A and B, and the deep reticulation involving *F. cronquistii* (C₃) and *F. robusta* (C₃). Also, it recovered a reticulation event (consistent with the 18-taxon dataset) where *F. vaginata* (C₄-like) and *F. kochiana* (C₄) within Clade A had a hybrid origin.

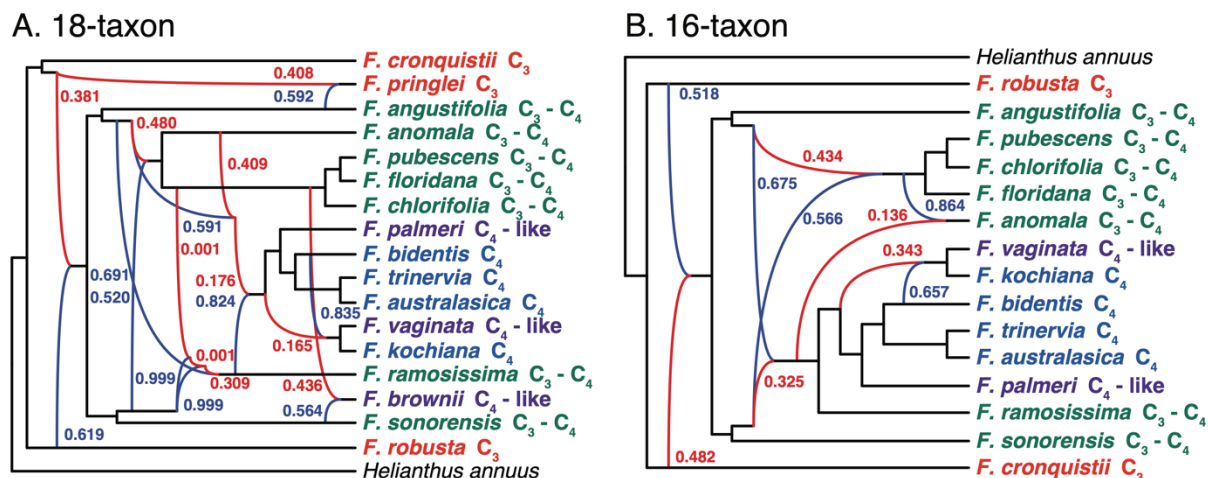


Fig. 2. *Flaveria* species networks with the best maximum pseudo-likelihood scores with PhyloNet for the (A) 18-taxon and (B) 16-taxon data sets. Species names are colored by photosynthetic type. Red and blue curved branches indicate the minor and major edges, respectively, of hybrid nodes. Numbers next to curved branches indicate inheritance probabilities for each hybrid node.

The HyDe analysis of all possible triples using the 17 species of *Flaveria* resulted in 2,040 hybridization tests, of which 311 triples were significant (Table S2). The analyses without *F. pringlei* (C_3) resulted in 247 significant hybridization tests of 1,680 overall tests (Table S3). HyDe analyses detected 12 species as potential hybrids (Fig. 3). These species included all members of Clade B which comprises five C_3 - C_4 and one C_4 -like species. Hybrids detected in Clade B had several potential parental lineages from across *Flaveria* and admixture (γ) values were either closer to zero or one (Fig. 3). *Flaveria chlorifolia*, *F. floridana*, *F. pubescens*, *F. anomala* showed similar hybridization patterns consistent with a single ancient hybrid origin of these species as shown in the PhyloNet analyses. On the other hand, *F. sonorensis* and *F. brownii* showed hybridization patterns different from the rest of the species of the clade, suggesting their independent hybrid origins as also seen in the PhyloNet analyses. In Clade A, and unlike PhyloNet, HyDe detected only four instances of hybridization. These included the C_3 - C_4 species *F. ramosissima* and the two C_4 -like species, *F. vaginata* and *F. palmeri*, of the clade.

365 In these three cases γ was consistent with ancient hybridization. *Flaveria vaginata* had notably
 366 fewer potential parental lineages suggesting a more recent reticulation event. The fourth species,
 367 *F. bidentis*, was the only C₄ member of the clade which was detected as a hybrid. In this case, all
 368 potential parental lineages are members of Clade A, and γ values around 0.5 suggested a recent
 369 reticulation event. Outside clades A and B, *F. angustifolia* (C₃-C₄) and *F. pringlei* (C₃) were
 370 detected as hybrids. In both cases, the potential parental lineages come from across *Flaveria* with
 371 γ values suggesting ancient reticulation. Overall, HyDe detected all C₃-C₄ and C₄-like species as
 372 well as *F. bidentis* (C₄) and *F. pringlei* (C₃) as potential ancient hybrids.

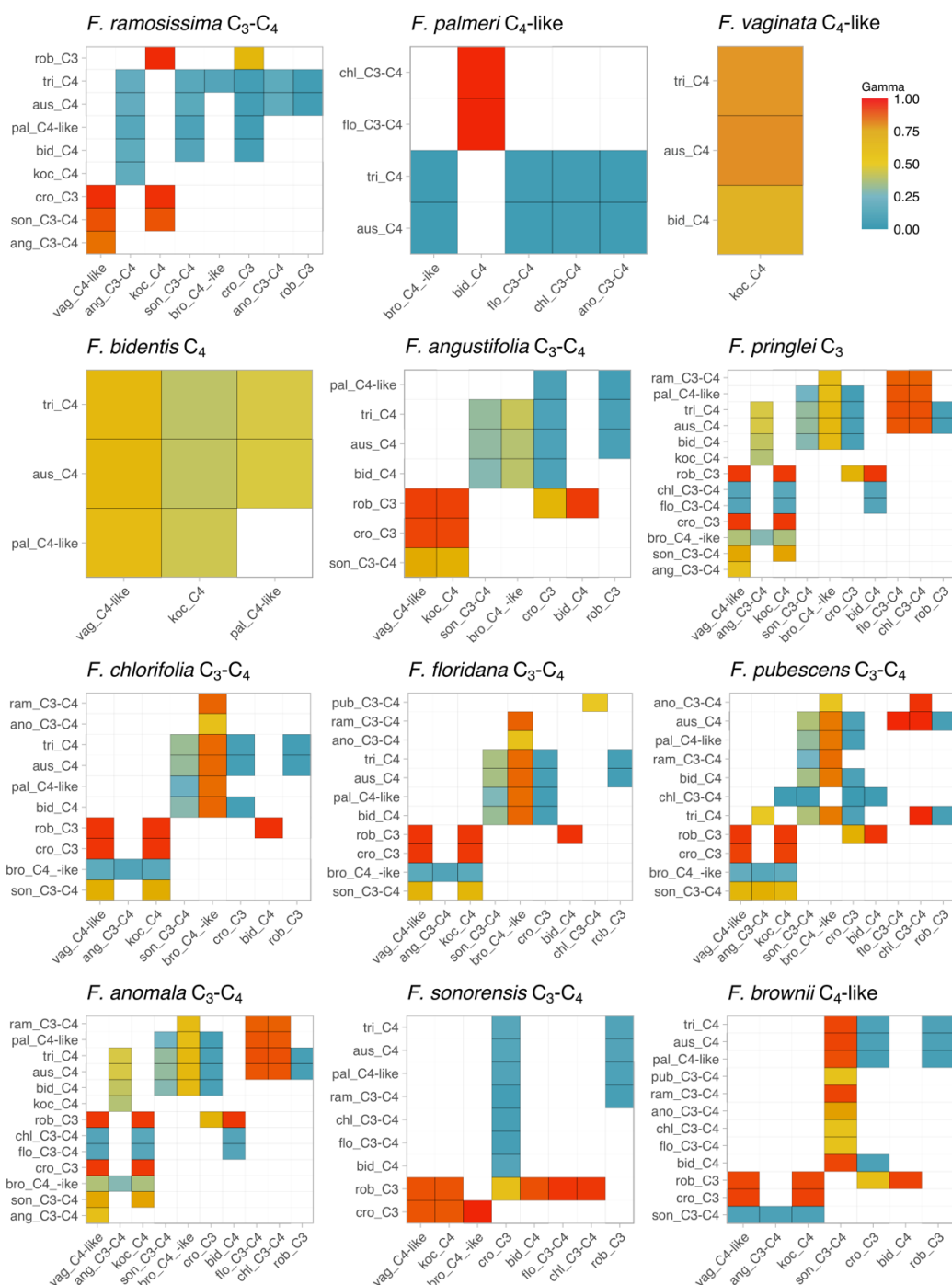


Fig. 3. HyDe significant hybridization test for the 12 species of *Flaveria* identified as potential hybrids. Species on the x-axis are parental lineage 1 (P1) and species on the y-axis are parental lineage 2 (P2). Only colored boxes denote possible combinations of P1 and P2 as parents of hybrid species. The color scale represents the value of the hybridization parameter γ for each hybridization event. Recent 50:50 hybrids would be represented by a $\gamma \sim 0.5$. Values of γ approaching 0 indicate a major hybrid contribution from P1, and values approaching 1 indicate a major hybrid contribution from P2, with both cases representing ancient hybridization.

Lack of whole genome duplications

The orthogroup mapping did not reveal any node in *Flaveria* with elevated levels of gene duplication (Fig S7), showing the absence of whole genome duplication in the genus. In part this is expected as *Flaveria* is consistently diploid (see Powell, 1978 and ref. therein) with a haploid chromosome number of $n = 18$. Furthermore, the lack of whole genome duplication in *Flaveria* suggests that reticulation events in this group are homoploid hybridizations.

DISCUSSION

In C_4 photosynthesis, high rates of net photosynthesis and a highly competitive water and nitrogen use efficiency are achieved by spatially separated carbon fixation in the outer mesophyll cells preceding the Calvin-Benson cycle, and by effectively fueling Rubisco with always high CO_2 concentration in the controlled seclusion of the Kranz cells (Long, 1999). Resulting low levels of photorespiration make C_4 plants competitive in various stressful environments where carbon deficiency poses a problem to C_3 plants (Sage et al., 2012). C_4 evolved more than 60 times in angiosperms with hotspots of C_4 origins in Poaceae and Amaranthaceae (Sage et al., 2018). Due to the anatomical and gene regulatory complexity of the C_4 pathway, it seems clear that there must have been intermediate stable phenotypes during the evolution of C_4 from a C_3 ancestor (Monson and Moore, 1989). The established generalized model of C_4 evolution tries to explain the sequence of intermediate adaptive events during the transition from the ancestral C_3 to C_4 using the naturally occurring C_3 - C_4 intermediate phenotypes of *Flaveria* (and other lineages) as proxies of intermediate stages in C_4 evolution (Sage et al., 2014; Bräutigam and Gowik, 2016). However, *Flaveria* is also known for rampant interfertility of its 21 (mostly diploid) species (Long and Rhamstine, 1968; Powell, 1978), and for the transferability of

photosynthetic traits to hybrid offspring in hybridization experiments (Apel et al., 1988; Kadereit et al., 2017 and ref. therein). Therefore, a clear understanding of the phylogenetic history of this model lineage of C₄ evolution, including tests for possible reticulate evolution, is fundamental as this might have strong implications for our understanding of the evolution of C₄ photosynthesis in general.

Our analyses using transcriptome data of 17 *Flaveria* species revealed rampant gene tree discordance along the backbone of the phylogeny as well as the clades containing most C₃-C₄ intermediate and C₄-like species (clades A and B; visualized in the cloudogram in Fig. 1). Coalescence simulations showed that gene tree discordance in *Flaveria* cannot be attributed to ILS alone. Our initial species network analyses including all 17 species sampled consistently identified *Flaveria brownii* (C₄-like) and *F. pringlei* (C₃) as hybrids (Figs. 2 and 3). After exclusion of these two most likely recent hybrids, deep reticulation events were recovered more clearly. The network analyses of the remaining species suggested an early reticulation event between two C₃ lineages (*F. robusta* and *F. cronquistii*) giving rise to the ancestor of the lineage containing all C₃-C₄ intermediate species, C₄-like species and C₄ species. This result is supported by the HyDe analysis which identified all C₃-C₄ and C₄-like species as potential ancient hybrids. The ancestors of *F. robusta* and *F. cronquistii* seem to have contributed equally to the origin of the hybrid lineage (Fig. 2). Within this lineage there exist two parental lineages, *F. angustifolia* (C₃-C₄) and *F. sonorensis* (C₃-C₄), that seem to have contributed to a robust clade containing all C₄ species plus *F. ramosissima* (C₃-C₄) and *F. vaginata* (C₄-like; clade A in Fig. 1), and also to another robust clade of four C₃-C₄ intermediate species (*F. pubescens*, *F. chlorifolia*, *F. floridana*, *F. anomala*; partial clade B in Fig. 1; supported also by the HyDe analysis). Of these four species, *F. anomala* was introgressed by the ancestor of clade A (Fig. 2).

These results have several important implications that will be discussed in the following three sections: 1) natural C₃-C₄ intermediates species in *Flaveria* do not seem to result from hybridization between a C₃ and a C₄ lineage (as similar C₃-C₄ intermediate phenotypes resulting from crossing experiments might suggest); 2) recurrent homoploid hybridization possibly played a major role in the evolution of C₄ photosynthesis in *Flaveria* with an initial hybridization event between two C₃ species (*F. robusta* and *F. cronquistii*) as a possible trigger, 3) only the ancestral lineages of *F. angustifolia* and *F. sonorensis* (both C₃-C₄ intermediates) seem to be involved in the formation of clades A and B, of which only clade A shows C₄ photosynthesis.

Hybridization is an important factor in plant evolution and speciation in general (Abbott et al., 2013) and *Flaveria* is no exception to this but also shows hybridization in a more complex way than we expected. From the phenotypic outcome of the numerous C₃ × C₄ hybridization experiments in *Flaveria* it was conceivable that naturally occurring C₃-C₄ intermediate species might be the result of crosses between parental lineages with different photosynthetic types (Monson and Moore, 1989; Kadereit et al., 2017). However, our results indicate that origin of C₃-C₄ intermediates might be more complex: in *Flaveria* there are several recent hybrids expressing intermediate or deviating phenotypes compared to the parental lineages which perturb phylogenetic reconstruction (in particular, *F. pringlei* and *F. brownii*). There also were ancient hybridization events challenging the reconstruction of the backbone (Fig. 1; see below). McKown et al. (2005) and Lyu et al., 2015 interpreted *F. brownii* as representing an independent and recent origin of C₄-like photosynthesis from C₃-C₄ ancestors. According to our analyses, *F. brownii* is a recent hybrid between *F. sonorensis* (C₃-C₄) and one of the other species in clade B (all C₃-C₄; Fig. 1–3), probably *F. floridana* with which it forms fertile F1 and F2 hybrids (Powell, 1978). This is an important finding for the interpretation of trait evolution in *Flaveria*.

The C₄-like photosynthesis in *F. brownii* seems to have resulted from a cross between a C₂ type I (*F. sonorensis*) and C₂ type 2 species (possibly *F. floridana*; see Table 1) resulting in stronger C₄-ness of *F. brownii*. Since *F. brownii* possesses C₃ isoforms of the key enzymes of the C₄ pathway (e.g., Kubien et al., 2008; Gowik and Westhoff, 2011; Ludwig, 2011), the C₄-like metabolism in *F. brownii* seems to have resulted from a highly effective gene regulatory change in comparison to its parental lineages rather than from the acquisition of C₄ isoforms. It clearly outcompetes its parental lineages in terms of C₄ physiology. Taniguchi et al. (2021), studying genome size evolution in *Flaveria*, showed dynamic alteration of genome size in the genus with *F. brownii* having the largest genome size among the 11 species investigated. Rewiring the parental genomes might have led to the C₄-like phenotype found in *F. brownii* and might have facilitated adaptive divergence resulting in colonization of the coastal flats and islands of the lower Texas Gulf Coast. Similarly, our analyses revealed *F. pringlei* (C₃ proto-kranz) as a recent hybrid between *F. cronquistii* (C₃) and *F. angustifolia* (C₃-C₄; Fig. 1-3). Therefore, the proto-kranz phenotype in this species might be of different origin than that of *F. robusta* (Table 1). In fact, Lyu et al. (2015) showed the *F. pringlei* sample used in their study to be of artificial hybrid origin (possibly resulting from unintended crosses in the greenhouse). Trait assessments in these two species, e.g., of leaf anatomical and ultrastructural traits (McKown and Dengler, 2007; Sage et al., 2013) might lead to re-evaluation of their assessment as evolutionary “basal” as they likely acquired the proto-kranz phenotype differently. Also, the similarities between *F. cronquistii* and *F. pringlei* found by McKown and Dengler (2007) and their differences to *F. robusta* can now be explained. According to our analyses, *F. robusta* and *F. cronquistii* seem to be representatives of ancient C₃ lineages in *Flaveria*, but not *F. pringlei*. The rare *Flaveria mcdougallii* (C₃, not represented in this analysis), which is morphologically and geographically distinct and might be

sister to all other species of *Flaveria* (Powell, 1978; McKown et al., 2005), would be an important species to add in further studies.

The most ancient hybridization event in *Flaveria* involved two C_3 lineages, *F. robusta* and *F. cronquistii*. According to Powell (1978), *Flaveria cronquistii* most closely resembles *F. robusta*. The two are geographically separated, and the former is distributed in the Tehuacán Valley region and the latter in Colima and Michoacán (both Mexico). There are no reports of artificial hybridization between these two species. The resulting ancient hybrid lineage seems to include all C_3 - C_4 intermediate, C_4 -like and C_4 species (Fig. 2; Table 1). Concerning leaf anatomy, *Flaveria robusta* differs from *F. cronquistii* by a higher vein density achieved through higher vein branching, and by a higher number of organelles in the bundle sheath cells where the organelles are located in a centripetal position along the cell wall connecting bundle sheath cells and vascular tissue. Organelles are more evenly distributed in *F. cronquistii*, and its leaves are more succulent and show larger bundle sheath cells (McKown and Dengler, 2007; Sage et al., 2013). The combination of these traits in a hybrid lineage and subsequent segregation effectively leading to a higher bundle sheath to mesophyll ratio and activated large bundle sheath cells may have triggered the evolution of “pre kranz” cells in *Flaveria*. Possibly the strong leaf anatomical differences between the two parental lineages promoted the origin of novel traits which then allowed this lineage to occupy new niches eco-geographically separate from the parents. There are multiple examples for plant lineages in which homoploid hybridization resulted in potentially adaptive genotypes through transgressive segregation, eventually leading to speciation (Gross and Rieseberg, 2005; Nieto Feliner et al., 2020). An increase of the bundle sheath to mesophyll ratio has been suggested to play an initial role in the evolution of C_4 in several plant lineages

(Marshall et al., 2007; McKown and Dengler, 2007; Christin et al., 2013; Griffiths et al., 2013; Lauterbach et al., 2019).

Two C₃-C₄ intermediate lineages, *F. angustifolia* and *F. sonorensis*, are involved in the formation of clades A and B according to our results. It is remarkable that only these two and not any other species (especially not the C₄-like species) contributed to the origin of these clades. In their extant distribution the two species do not overlap. *Flaveria angustifolia* grows in sclerophyllous scrub in Puebla and Oaxaca, while *F. sonorensis* is found only in the short-tree forests of tropical Sonora (Powell, 1978). Looking more closely at these two descendants of the lineages that seem to have hybridized in the past and possibly gave rise to C₄ photosynthesis might give new insights into important preconditions for the evolution of C₄ in *Flaveria*. Both *F. angustifolia* and *F. sonorensis* were categorized as C₂ Type I species (Table 1), but with weaker C₂ photosynthesis (relatively high amounts of glycine decarboxylase in the mesophyll cells and relatively high CO₂ compensation points) than other C₂ species of *Flaveria* (Sage et al., 2018). This finding implies the evolution of a C₂ phenotype prior to C₄, supporting the ‘photorespiratory bridge hypothesis’ (Sage et al., 2018) in case of *Flaveria*. However, it seems that C₄ evolution in *Flaveria* was triggered by hybridization of C₂ lineages, a scenario never suggested before. For *Flaveria* this somewhat shifts the focus to C₂ photosynthesis and under which selective conditions this type of photosynthesis might have evolved. To gain further insights into the evolution of C₂ photosynthesis, detailed studies of the origin, anatomy, and ecophysiology of *F. angustifolia* and *F. sonorensis* might be rewarding. Organelle enrichment and their flux-optimized positioning as well as glycine decarboxylase accumulation in the proto-kranz cells (Khoshhravesh et al., 2016) seem to be essential for C₂ photosynthesis (in eudicots and monocots). These traits enable species to more efficiently re-cycle respired CO₂ and to longer

maintain a positive assimilation rate under carbon deficient conditions. Since the majority of C_4 lineages do not have any known C_2 relatives (see Sage et al., 2018 for an overview), and C_2 lineages without close C_4 relative are known as well (see Lundgren, 2020 for an overview), the question remains whether there exist several evolutionary pathways to C_4 photosynthesis (Edwards, 2019), and whether C_2 should be considered an independent carbon concentrating mechanism not necessarily always intimately connected to C_4 photosynthesis (Lundgren, 2020 and ref. therein). Finally, a C_2 lineage might also be the result of ancient hybridization of a C_3 and a C_4 lineage, as has been suggested for *Salsola divaricata*, which then might have thrived through the large plasticity of photosynthetic traits inherited from photosynthetically divergent parental lineages (Tefarikis et al., 2021).

CONCLUSIONS

The young genus *Flaveria* which includes four C_3 , four C_4 , three C_4 -like and c. ten C_3 - C_4 intermediate species is remarkable for the high number of evolutionary reticulations creating an enormous diversity of phenotypes with different photosynthetic traits. Due to this and its strictly diploid chromosome number the genus is a highly interesting system to study the genetic basis of the C_4 syndrome and the role of transgressive segregation in the origin of genotypes eventually leading to the evolution of C_4 photosynthesis. We found evidence that homoploid hybridization of C_3 lineages might have triggered the evolution of C_2 photosynthesis, and that homoploid hybridization of C_2 lineages gave rise to C_4 -like or C_4 photosynthesis. In both cases the hybrid derivatives possibly surpassed the parental performance under conditions of high photorespiration and had an adaptive advantage. However, since reticulation occurred in recent as well as ancient lineages of the genus, the sequence of evolutionary events needs to be studied

541 in the light of a carefully reconstructed phylogenetic history of the genus. Comparison of the
542 entire genomes of parental and hybrid lineages should allow us to detect whether the origin of
543 new photosynthetic traits is indeed the result of transgressive segregation (de los Reyes, 2019),
544 as suggested here, or of stepwise mutational change of relevant genes.
545

546 DATA AVAILABILITY STATEMENT

547 Analysis and results files can be accessed at the Dryad repository XXXX

548

549 CONFLICT OF INTEREST

550 The authors declare no conflict of interest.

551

552 AUTHOR CONTRIBUTIONS

553 GK and DFM-B conceived the study. DFM-B performed all analyses. GK and DFM-B evaluated
554 the results and wrote the paper.

555

556 FUNDING

557 Financial support for this study came from LMU Munich and the German Science Foundation
558 (DFG grant KA1816/9-1).

559

560 ACKNOWLEDGMENTS

561 We thank Joachim W. Kadereit (Mainz) for valuable comments on the manuscript.

562

563

564

565

566

567

SUPPLEMENTARY MATERIAL

Table S1. Taxon sampling and source of data

Table S2. HyDe significant hybridization tests for all species of *Flaveria*.

Table S3. HyDe significant hybridization tests for all species of *Flaveria* excluding *F. pringlei* (C₃).

Fig. S1. A. Maximum likelihood phylogeny of *Flaveria* inferred with IQ-TREE from the concatenated 1249-nuclear gene supermatrix. Numbers above branches represent bootstrap support (BS). Branch lengths as substitutions per site (scale bar on the bottom). B. ASTRAL tree of *Flaveria* inferred from the 1,295 nuclear gene trees. Local posterior probabilities (LLP) are shown next to nodes. Internal branch lengths are in coalescent units (scale bar on the bottom).

Fig. S2. A. Maximum likelihood cladogram of *Flaveria* inferred with IQ-TREE from the concatenated 1249-nuclear gene supermatrix. B. ASTRAL cladogram of *Flaveria* inferred from the 1,295 nuclear gene trees. Pie charts represent the proportion of gene trees that support that clade (blue), the main alternative bifurcation (green), the remaining alternatives (red), and conflict or support that have <50% bootstrap support (gray). Number above and below branches represent the number of concordant and discordant informative gene trees, respectively.

Fig. S3. A. Maximum likelihood cladogram of *Flaveria* inferred with IQ-TREE from the concatenated 1249-nuclear gene supermatrix. B. ASTRAL cladogram of *Flaveria* inferred from

the 1,295 nuclear gene trees. Quartet Sampling (QS) scores are shown above branches. QS scores: Quartet concordance/Quartet differential/Quartet informativeness. Circles at nodes are colored by quartet concordance support.

Fig. S4. Distribution of tree-to-tree distances between empirical gene trees and the ASTRAL tree, compared to the distribution of tree-to-tree distances between simulated trees and the ASTRAL tree.

Fig. S5. Maximum pseudo-likelihood scores for species networks inferred with PhyloNet using the (A) 18-taxon, (B) and 16-taxon data sets. The x-axis notes the maximum number of reticulations for each of the network searches allowing up to ten reticulation events.

Fig. S6. Maximum pseudo-likelihood species networks inferred with PhyloNet using the (A) 18-taxon, (B) and 16-taxon data sets and allowing up to ten reticulation events. Red and blue curved branches indicate the minor and major edges, respectively of hybrid nodes. Numbers next to curved branches indicate inheritance probabilities for each hybrid node.

Fig. S7. Maximum likelihood cladogram of *Flaveria* inferred with IQ-TREE from the concatenated 1249-nuclear gene supermatrix. Numbers above branches are gene duplication counts and numbers below branches are gene duplication percentages.

REFERENCES

- Abbott, R., Albach, D., Ansell, S., Arntzen, J. W., Baird, S. J. E., Bierne, N., et al. (2013). Hybridization and speciation. *Journal of Evolutionary Biology* 26, 229–246. doi:10.1111/j.1420-9101.2012.02599.x.
- Anderberg, A. A., Baldwin, B. G., Bayer, R. G., Breitwieser, J., Jeffrey, C., Dillon, M. O., et al. (2007). “Compositae,” in *Flowering plants · Eudicots: Asterales*, eds. J. W. Kadereit and C. Jeffrey (Berlin, Heidelberg: Springer Berlin Heidelberg), 61–588. doi:10.1007/978-3-540-31051-8_7.
- Apel, P., Bauwe, H., Bassüner, B., and Maass, I. (1988). Photosynthetic properties of *Flaveria cronquistii*, *F. palmeri*, and hybrids between them. *Biochemie und Physiologie der Pflanzen* 183, 291–299. doi:10.1016/S0015-3796(88)80021-0.
- Apel, P., and Maass, I. (1981). Photosynthesis in species of *Flaveria* CO₂ compensation concentration, O₂ influence on photosynthetic gas exchange and $\delta^{13}\text{C}$ values in species of *Flaveria* (Asteraceae). *Biochemie und Physiologie der Pflanzen* 176, 396–399. doi:10.1016/S0015-3796(81)80052-2.
- Blair, C., and Ané, C. (2020). Phylogenetic trees and networks can serve as powerful and complementary approaches for analysis of genomic data. *Systematic Biology* 69, 593–601. doi:10.1093/sysbio/syz056.
- Blischak, P. D., Chifman, J., Wolfe, A. D., and Kubatko, L. S. (2018). HyDe: A python package for genome-scale hybridization detection. *Systematic Biology* 67, 821–829. doi:10.1093/sysbio/syy023.
- Bolger, A. M., Lohse, M., and Usadel, B. (2014). Trimmomatic - a flexible trimmer for Illumina sequence data. *Bioinformatics* 30, 2112–2120. doi:10.1093/bioinformatics/btu170/-/DC1.

635 Bräutigam, A., and Gowik, U. (2016). Photorespiration connects C₃ and C₄ photosynthesis.
636 *Journal of Experimental Botany* 67, 2953–2962. doi:10.1093/jxb/erw056.

637 Brown, J. W., Walker, J. F., and Smith, S. A. (2017). Phyx - phylogenetic tools for unix.
638 *Bioinformatics* 33, 1886–1888. doi:10.1093/bioinformatics/btx063/-/DC1.

639 Chen, L.-Y., Morales-Briones, D. F., Passow, C. N., and Yang, Y. (2019). Performance of gene
640 expression analyses using de novo assembled transcripts in polyploid species.
641 *Bioinformatics*. doi:10.1093/bioinformatics/btz620.

642 Christin, P.-A., Osborne, C. P., Chatelet, D. S., Columbus, J. T., Besnard, G., Hodkinson, T. R.,
643 et al. (2013). Anatomical enablers and the evolution of C₄ photosynthesis in grasses. *Proc*
644 *Natl Acad Sci USA* 110, 1381. doi:10.1073/pnas.1216777110.

645 Cloutier, A., Sackton, T. B., Grayson, P., Clamp, M., Baker, A. J., and Edwards, S. V. (2019).
646 Whole-genome analyses resolve the phylogeny of flightless birds (Palaeognathae) in the
647 presence of an empirical anomaly zone. *Systematic Biology* 68, 937–955.
648 doi:10.1093/sysbio/syz019.

649 Davidson, N. M., and Oshlack, A. (2014). Corset: enabling differential gene expression analysis
650 for de novo assembled transcriptomes. *Genome Biology* 15, 57. doi:10.1186/s13059-014-
651 0410-6.

652 de los Reyes, B. G. (2019). Genomic and epigenomic bases of transgressive segregation – New
653 breeding paradigm for novel plant phenotypes. *Plant Science* 288, 110213.
654 doi:10.1016/j.plantsci.2019.110213.

655 Degnan, J. H., and Rosenberg, N. A. (2009). Gene tree discordance, phylogenetic inference and
656 the multispecies coalescent. *Trends in Ecology & Evolution* 24, 332–340.
657 doi:10.1016/j.tree.2009.01.009.

658 Doyle, J. J. (1992). Gene trees and species trees: Molecular systematics as one-character
659 taxonomy. *Systematic Botany* 17, 144. doi:10.2307/2419070.

660 Durand, E. Y., Patterson, N., Reich, D., and Slatkin, M. (2011). Testing for ancient admixture
661 between closely related populations. *Molecular Biology and Evolution* 28, 2239–2252.
662 doi:10.1093/molbev/msr048.

663 Edwards, E. J. (2019). Evolutionary trajectories, accessibility and other metaphors: the case of C₄
664 and CAM photosynthesis. *New Phytologist* 223, 1742–1755. doi:10.1111/nph.15851.

665 Fu, L., Niu, B., Zhu, Z., Wu, S., and Li, W. (2012). CD-HIT: accelerated for clustering the next-
666 generation sequencing data. *Bioinformatics* 28, 3150–3152.
667 doi:10.1093/bioinformatics/bts565.

668 Galtier, N., and Daubin, V. (2008). Dealing with incongruence in phylogenomic analyses.
669 *Philosophical Transactions of the Royal Society B: Biological Sciences* 363, 4023–4029.
670 doi:10.1098/rstb.2008.0144.

671 Giraud, T., Refrégier, G., Le Gac, M., de Vienne, D. M., and Hood, M. E. (2008). Speciation in
672 fungi. *Fungal Genetics and Biology* 45, 791–802. doi:10.1016/j.fgb.2008.02.001.

673 Gowik, U., and Westhoff, P. (2011). “C₄-Phosphoenolpyruvate Carboxylase,” in *C₄*
674 *Photosynthesis and Related CO₂ Concentrating Mechanisms*, eds. A. S. Raghavendra and
675 R. F. Sage (Dordrecht: Springer Netherlands), 257–275. doi:10.1007/978-90-481-9407-
676 0_13.

677 Grabherr, M. G., Haas, B. J., Yassour, M., Levin, J. Z., Thompson, D. A., Amit, I., et al. (2011).
678 Full-length transcriptome assembly from RNA-Seq data without a reference genome.
679 *Nature Biotechnology* 29, 644–652. doi:10.1038/nbt.1883.

680 Green, R. E., Krause, J., Briggs, A. W., Maricic, T., Stenzel, U., Kircher, M., et al. (2010). A
681 draft sequence of the neandertal Genome. *Science* 328, 710–722.
682 doi:10.1126/science.1188021.

683 Griffiths, H., Weller, S. G., Toy, L. F. M., and Dennis, R. J. (2013). You’re so vein: Bundle
684 sheath physiology, phylogeny and evolution in C₃ and C₄ plants. *Plant, Cell &*
685 *Environment* 36, 249–261. doi:10.1111/j.1365-3040.2012.02585.x.

686 Gross, B. L., and Rieseberg, L. H. (2005). The ecological genetics of homoploid hybrid
687 speciation. *Journal of Heredity* 96, 241–252. doi:10.1093/jhered/esi026.

688 Haas, B. J., Papanicolaou, A., Yassour, M., Grabherr, M., Blood, P. D., Bowden, J., et al. (2013).
689 *De novo* transcript sequence reconstruction from RNA-seq using the Trinity platform for
690 reference generation and analysis. *Nature Protocols* 8, 1494–1512.
691 doi:10.1038/nprot.2013.084.

692 Kadereit, G., Bohley, K., Lauterbach, M., Tefarikis, D. T., and Kadereit, J. W. (2017). C₃-C₄
693 intermediates may be of hybrid origin – a reminder. *New Phytologist* 215, 70–76.
694 doi:10.1111/nph.14567.

695 Kalyaanamoorthy, S., Minh, B. Q., Wong, T. K. F., von Haeseler, A., and Jermini, L. S. (2017).
696 ModelFinder: fast model selection for accurate phylogenetic estimates. *Nat Methods* 14,
697 587–589. doi:10.1038/nmeth.4285.

698 Khoshravesh, R., Stinson, C. R., Stata, M., Busch, F. A., Sage, R. F., Ludwig, M., et al. (2016).
699 C₃-C₄ intermediacy in grasses: organelle enrichment and distribution, glycine
700 decarboxylase expression, and the rise of C₂ photosynthesis. *Journal of Experimental*
701 *Botany* 67, 3065–3078. doi:10.1093/jxb/erw150.

702 Ku, M. S. B., Monson, R. K., Littlejohn, R. O., Jr., Nakamoto, H., Fisher, D. B., and Edwards, G.
703 E. (1983). Photosynthetic characteristics of C₃-C₄ intermediate *Flaveria* species 1: I. Leaf
704 anatomy, photosynthetic responses to O₂ and CO₂, and activities of key enzymes in the
705 C₃ and C₄ pathways. *Plant Physiology* 71, 944–948. doi:10.1104/pp.71.4.944.

706 Ku, M. S. B., Wu, J., Dai, Z., Scott, R. A., Chu, C., and Edwards, G. E. (1991). Photosynthetic
707 and photorespiratory characteristics of *Flaveria* species 1. *Plant Physiology* 96, 518–528.
708 doi:10.1104/pp.96.2.518.

709 Kubatko, L. S., and Chifman, J. (2019). An invariants-based method for efficient identification
710 of hybrid species from large-scale genomic data. *BMC Evol Biol* 19, 112.
711 doi:10.1186/s12862-019-1439-7.

712 Kubien, D. S., Whitney, S. M., Moore, P. V., and Jesson, L. K. (2008). The biochemistry of
713 Rubisco in *Flaveria*. *Journal of Experimental Botany* 59, 1767–1777.
714 doi:10.1093/jxb/erm283.

715 Lanfear, R., Calcott, B., Ho, S. Y. W., and Guindon, S. (2012). PartitionFinder: Combined
716 selection of partitioning schemes and substitution models for phylogenetic analyses.
717 *Molecular Biology and Evolution* 29, 1695–1701. doi:10.1093/molbev/mss020.

718 Langmead, B., and Salzberg, S. L. (2012). Fast gapped-read alignment with Bowtie 2. *Nature*
719 *Methods* 9, 357–359. doi:10.1038/nmeth.1923.

720 Lauterbach, M., Zimmer, R., Alexa, A. C., Adachi, S., Sage, R., Sage, T., et al. (2019). Variation
721 in leaf anatomical traits relates to the evolution of C₄ photosynthesis in Tribuloideae
722 (Zygophyllaceae). *Perspectives in Plant Ecology, Evolution and Systematics* 39, 125463.
723 doi:10.1016/j.ppees.2019.125463.

724 Liu, L., and Yu, L. (2010). Phybase: an R package for species tree analysis. *Bioinformatics* 26,
725 962–963. doi:10.1093/bioinformatics/btq062.

726 Long, R. W., and Rhamstine, E. L. (1968). Evidence for the hybrid origin of *Flaveria latifolia*
727 (Compositae). *Brittonia* 20, 238–250. doi:10.2307/2805449.

728 Long, S. P. (1999). “Environmental Responses,” in *C₄ Plant Biology*, eds. R. F. Sage and R. K.
729 Monson (San Diego: Academic Press), 215–249. doi:10.1016/B978-012614440-6/50008-
730 2.

731 Ludwig, M. (2011). The molecular evolution of β -carbonic anhydrase in *Flaveria*. *Journal of*
732 *Experimental Botany* 62, 3071–3081. doi:10.1093/jxb/err071.

733 Lyu, M.-J. A., Gowik, U., Kelly, S., Covshoff, S., Hibberd, J. M., Sage, R. F., et al. (2021). The
734 coordination of major events in C₄ photosynthesis evolution in the genus *Flaveria*.
735 *Scientific Reports* 11, 15618. doi:10.1038/s41598-021-93381-8.

736 Lyu, M.-J. A., Gowik, U., Kelly, S., Covshoff, S., Mallmann, J., Westhoff, P., et al. (2015).
737 RNA-Seq based phylogeny recapitulates previous phylogeny of the genus *Flaveria*
738 (Asteraceae) with some modifications. *BMC Evolutionary Biology* 15, 116.
739 doi:10.1186/s12862-015-0399-9.

740 Mai, U., and Mirarab, S. (2018). TreeShrink: fast and accurate detection of outlier long branches
741 in collections of phylogenetic trees. *BMC Genomics* 19, 272. doi:10.1186/s12864-018-
742 4620-2.

743 Mandel, J. R., Dikow, R. B., Siniscalchi, C. M., Thapa, R., Watson, L. E., and Funk, V. A.
744 (2019). A fully resolved backbone phylogeny reveals numerous dispersals and explosive
745 diversifications throughout the history of Asteraceae. *Proc Natl Acad Sci USA* 116,
746 14083–14088. doi:10.1073/pnas.1903871116.

- 747 Marshall, D. M., Muhaidat, R., Brown, N. J., Liu, Z., Stanley, S., Griffiths, H., et al. (2007).
748 *Cleome*, a genus closely related to *Arabidopsis*, contains species spanning a
749 developmental progression from C₃ to C₄ photosynthesis. *The Plant Journal* 51, 886–896.
750 doi:10.1111/j.1365-313X.2007.03188.x.
- 751 Maureira-Butler, I. J., Pfeil, B. E., Muangprom, A., Osborn, T. C., and Doyle, J. J. (2008). The
752 reticulate history of *Medicago* (Fabaceae). *Systematic Biology* 57, 466–482.
753 doi:10.1080/10635150802172168.
- 754 McKown, A. D., and Dengler, N. G. (2007). Key innovations in the evolution of Kranz anatomy
755 and C₄ vein pattern in *Flaveria* (Asteraceae). *American Journal of Botany* 94, 382–399.
756 doi:10.3732/ajb.94.3.382.
- 757 McKown, A. D., Moncalvo, J.-M., and Dengler, N. G. (2005). Phylogeny of *Flaveria*
758 (Asteraceae) and inference of C₄ photosynthesis evolution. *American Journal of Botany*
759 92, 1911–1928. doi:10.3732/ajb.92.11.1911.
- 760 Minh, B. Q., Schmidt, H. A., Chernomor, O., Schrempf, D., Woodhams, M. D., von Haeseler,
761 A., et al. (2020). IQ-TREE 2: New models and efficient methods for phylogenetic
762 inference in the genomic era. *Molecular Biology and Evolution* 37, 1530–1534.
763 doi:10.1093/molbev/msaa015.
- 764 Monson, R. K., and Moore, B. D. (1989). On the significance of C₃-C₄ intermediate
765 photosynthesis to the evolution of C₄ photosynthesis. *Plant, Cell & Environment* 12, 689–
766 699. doi:10.1111/j.1365-3040.1989.tb01629.x.
- 767 Morales-Briones, D. F., Kadereit, G., Tefarikis, D. T., Moore, M. J., Smith, S. A., Brockington,
768 S. F., et al. (2021). Disentangling sources of gene tree discordance in phylogenomic data

769 sets: Testing ancient hybridizations in Amaranthaceae s.l. *Systematic Biology* 70, 219–
770 235. doi:10.1093/sysbio/syaa066.

771 Nakamoto, H., Ku, M. S. B., and Edwards, G. E. (1983). Photosynthetic characteristics of C₃-C₄
772 intermediate *Flaveria* species II. Kinetic properties of phosphoenolpyruvate carboxylase
773 from C₃, C₄ and C₃-C₄ intermediate species. *Plant and Cell Physiology* 24, 1387–1393.
774 doi:10.1093/oxfordjournals.pcp.a076659.

775 Nieto Feliner, G., Casacuberta, J., and Wendel, J. F. (2020). Genomics of evolutionary novelty in
776 hybrids and polyploids. *Frontiers in Genetics* 11, 792. Available at:
777 <https://www.frontiersin.org/article/10.3389/fgene.2020.00792>.

778 Pamilo, P., and Nei, M. (1988). Relationships between gene trees and species trees. *Molecular*
779 *Biology and Evolution* 5, 568–583. doi:10.1093/oxfordjournals.molbev.a040517

780 Patro, R., Duggal, G., Love, M. I., Irizarry, R. A., and Kingsford, C. (2017). Salmon provides
781 fast and bias-aware quantification of transcript expression. *Nature Methods* 14, 417–419.
782 doi:10.1038/nmeth.4197.

783 Payseur, B. A., and Rieseberg, L. H. (2016). A genomic perspective on hybridization and
784 speciation. *Molecular Ecology* 25, 2337–2360. doi:10.1111/mec.13557.

785 Pease, J. B., Brown, J. W., Walker, J. F., Hinchliff, C. E., and Smith, S. A. (2018). Quartet
786 Aampling distinguishes lack of support from conflicting support in the green plant tree of
787 life. *American Journal of Botany* 105, 385–403. doi:10.1002/ajb2.1016.

788 Powell, A. M. (1978). Systematics of *Flaveria* (Flaveriinae--Asteraceae). *Annals of the Missouri*
789 *Botanical Garden* 65, 590–636. doi:10.2307/2398862.

790 Pruitt, K. D., Tatusova, T., and Maglott, D. R. (2007). NCBI reference sequences (RefSeq): a
791 curated non-redundant sequence database of genomes, transcripts and proteins. *Nucleic*
792 *Acids Research* 35, D61–D65. doi:10.1093/nar/gkl842.

793 R Core Team. 2021. R: A language and environment for statistical computing. R foundation for
794 statistical computing, Vienna, Austria. URL <https://www.R-project.org/>.

795 Rannala, B., and Yang, Z. (2003). Bayes estimation of species divergence times and ancestral
796 population sizes using DNA sequences from multiple loci. *Genetics* 166, 1645–1656. doi:
797 10.1093/genetics/164.4.1645.

798 Robinson, D. F., and Foulds, L. R. (1981). Comparison of phylogenetic trees. *Mathematical*
799 *Biosciences* 53, 131–147. doi:10.1016/0025-5564(81)90043-2.

800 Sage, R. F., Khoshraves, R., and Sage, T. L. (2014). From proto-Kranz to C₄ Kranz: Building
801 the bridge to C₄ photosynthesis. *Journal of Experimental Botany* 65, 3341–3356.
802 doi:10.1093/jxb/eru180.

803 Sage, R. F., Monson, R. K., Ehleringer, J. R., Adachi, S., and Pearcy, R. W. (2018). Some like it
804 hot: the physiological ecology of C₄ plant evolution. *Oecologia* 187, 941–966.
805 doi:10.1007/s00442-018-4191-6.

806 Sage, R. F., Sage, T. L., and Kocacinar, F. (2012). Photorespiration and the evolution of C₄
807 photosynthesis. *Annu. Rev. Plant Biol.* 63, 19–47. doi:10.1146/annurev-arplant-042811-
808 105511.

809 Sage, T. L., Busch, F. A., Johnson, D. C., Friesen, P. C., Stinson, C. R., Stata, M., et al. (2013).
810 Initial events during the evolution of C₄ photosynthesis in C₃ species of *Flaveria*. *Plant*
811 *Physiology* 163, 1266–1276. doi:10.1104/pp.113.221119.

812 Sayyari, E., and Mirarab, S. (2016). Fast coalescent-based computation of local branch support
813 from quartet frequencies. *Molecular Biology and Evolution* 33, 1654–1668.
814 doi:10.1093/molbev/msw079.

815 Schliep, K. P. (2011). phangorn: phylogenetic analysis in R. *Bioinformatics* 27, 592–593.
816 doi:10.1093/bioinformatics/btq706.

817 Schwenk, K., Brede, N., and Streit, B. (2008). Introduction. Extent, processes and evolutionary
818 impact of interspecific hybridization in animals. *Philosophical Transactions of the Royal*
819 *Society B: Biological Sciences* 363, 2805–2811. doi:10.1098/rstb.2008.0055.

820 Scornavacca, C., Belkhir, K., Lopez, J., Dernas, R., Delsuc, F., Douzery, E. J. P., et al. (2019).
821 OrthoMaM v10: Scaling-up orthologous coding sequence and exon alignments with more
822 than one hundred mammalian Genomes. *Molecular Biology and Evolution* 36, 861–862.
823 doi:10.1093/molbev/msz015.

824 Smith, B. N., and Turner, B. L. (1975). Distribution of Kranz syndrome among asteraceae.
825 *American Journal of Botany* 62, 541–545. doi:10.2307/2441964.

826 Smith, S. A., Moore, M. J., Brown, J. W., and Yang, Y. (2015). Analysis of phylogenomic
827 datasets reveals conflict, concordance, and gene duplications with examples from animals
828 and plants. *BMC Evolutionary Biology* 15, 150. doi:10.1186/s12862-015-0423-0.

829 Smith, S. A., and O’Meara, B. C. (2012). treePL: divergence time estimation using penalized
830 likelihood for large phylogenies. *Bioinformatics* 28, 2689–2690.
831 doi:10.1093/bioinformatics/bts492.

832 Smith-Unna, R., Boursnell, C., Patro, R., Hibberd, J. M., and Kelly, S. (2016). TransRate:
833 reference-free quality assessment of de novo transcriptome assemblies. *Genome Research*
834 26, 1134–1144. doi:10.1101/gr.196469.115.

835 Solís-Lemus, C., and Ané, C. (2016). Inferring phylogenetic networks with maximum
836 pseudolikelihood under incomplete lineage sorting. *PLoS Genetics* 12, e1005896-21.
837 doi:10.1371/journal.pgen.1005896.

838 Soltis, P. S., and Soltis, D. E. (2009). The role of hybridization in plant speciation. *Annu. Rev.*
839 *Plant Biol.* 60, 561–588. doi:10.1146/annurev.arplant.043008.092039.

840 Song, L., and Florea, L. (2015). Rcorrector: efficient and accurate error correction for Illumina
841 RNA-seq reads. *GigaScience* 4. doi:10.1186/s13742-015-0089-y.

842 Stamatakis, A. (2014). RAxML version 8 - a tool for phylogenetic analysis and post-analysis of
843 large phylogenies. *Bioinformatics* 30, 1312–1313. doi:10.1093/bioinformatics/btu033/-
844 /DC1.

845 Swofford, D. (2002). PAUP*. Phylogenetic analysis using parsimony (*and other methods)
846 version 4. *Sunderland, MA: Sinauer Associates*.

847 Taniguchi, Y. Y., Gowik, U., Kinoshita, Y., Kishizaki, R., Ono, N., Yokota, A., et al. (2021).
848 Dynamic changes of genome sizes and gradual gain of cell-specific distribution of C₄
849 enzymes during C₄ evolution in genus *Flaveria*. *The Plant Genome* 14, e20095.
850 doi:10.1002/tpg2.20095.

851 Tefarikis, D. T., Morales-Briones, D. F., Yang, Y., Edwards, G., and Kadereit, G. (2021). On the
852 hybrid origin of the C₂ *Salsola divaricata* agg. (Amaranthaceae) from C₃ and C₄ parental
853 lineages. *bioRxiv*, 2021.09.23.461503. doi:10.1101/2021.09.23.461503.

854 Than, C., Ruths, D., and Nakhleh, L. (2008). PhyloNet: a software package for analyzing and
855 reconstructing reticulate evolutionary relationships. *BMC Bioinformatics* 9, 322–16.
856 doi:10.1186/1471-2105-9-322.

857 van Dongen, S. M. (2000). Graph Clustering by Flow Simulation. Available at:
858 <https://dl.acm.org/citation.cfm?id=868979>.

859 Wen, D., Yu, Y., Zhu, J., and Nakhleh, L. (2018). Inferring phylogenetic networks using
860 PhyloNet. *Systematic Biology* 67, 735–740. doi:10.1093/sysbio/syy015.

861 Yang, Y., Moore, M. J., Brockington, S. F., Mikenas, J., Olivieri, J., Walker, J. F., et al. (2018).
862 Improved transcriptome sampling pinpoints 26 ancient and more recent polyploidy events
863 in Caryophyllales, including two allopolyploidy events. *New Phytologist* 217, 855–870.
864 doi:10.1111/nph.14812.

865 Yang, Y., and Smith, S. A. (2013). Optimizing *de novo* assembly of short-read RNA-seq data for
866 phylogenomics. *BMC Genomics* 14, 328. doi:10.1186/1471-2164-14-328.

867 Yang, Y., and Smith, S. A. (2014). Orthology inference in nonmodel organisms using
868 transcriptomes and low-coverage genomes: Improving accuracy and matrix occupancy for
869 phylogenomics. *Molecular Biology and Evolution* 31, 3081–3092.
870 doi:10.1093/molbev/msu245.

871 Yu, Y., and Nakhleh, L. (2015). A maximum pseudo-likelihood approach for phylogenetic
872 networks. *BMC Genomics* 16, S10. doi:10.1186/1471-2164-16-S10-S10.

873 Zhang, C., Rabiee, M., Sayyari, E., and Mirarab, S. (2018). ASTRAL-III: polynomial time
874 species tree reconstruction from partially resolved gene trees. *BMC Bioinformatics* 19,
875 153. doi:10.1186/s12859-018-2129-y.